From phasing to structure refinement in-house: Cr/Cu dual wavelength system and a loopless free crystal mounting method

Nobuhisa Watanabe

Division of Biological Sciences, Graduate School of Science, Hokkaido University, Japan, and Photon Factory, Institute of Materials Structure Science, High Energy Accelerator Research Organization, Japan.
E-mail: nobuhisa@sci.hokudai.ac.jp

Synopsis Examples of Cr SAD structure solutions using a Cr/Cu dual wavelength system in combination with a loopless free crystal mounting method are shown.

Abstract The practical applicability of in-house structure determination using Cr *K*α X-rays (2.29 Å) and a loopless free crystal mounting method was examined using five novel proteins. Proteins from 9.6 kDa to 84 kDa have been solved using this method without any derivatization. In all cases, more than 90% of all the structures were constructed automatically with side chains by use of the Cr SAD method. The free crystal mounting technique increases the accuracy of the anomalous differences between the Bijvoet mates, and makes the in-house single-wavelength SAD method with a Cr *K*α X-ray source a very useful tool for high-throughput structure determination. In addition, a Cr/Cu dual wavelength system makes it possible to perform structure analysis from phasing to refinement of the structure in-house.

Keywords: Cr radiation; SAD method; free crystal mounting method

1. Introduction

Single-wavelength anomalous diffraction (SAD) phasing has become a useful tool for protein structure determination (Rice *et al.*, 2000; Dauter *et al.*, 2002; Blow, 2003). The choice of X-ray wavelength is one of the major decisions required for SAD data collection (Mueller-Dieckmann *et al.*, 2005). However, changing the wavelength is not possible for in-house X-ray sources. In the laboratory, we can only choose from several anticathode targets such as Cu *K*α (1.54 Å), Co *K*α (1.79 Å) and Cr *K*α (2.29 Å). By utilizing the longer wavelength, the small anomalous signals generated from small atomic weight or 'light' atoms such as sulfur can be enhanced to a level where they can be used to phase macromolecular structures. For example, the anomalous scattering factor of sulfur increases from 0.56 e^- at Cu *K*α to 1.14 e^- at Cr *K*α. Considering the phasing using the anomalous signal of such weak anomalous scatterers in underivatized native protein, the longer wavelength of Cr *K*α X-rays may be the optimal choice for these experiments (Wang, 1985; Kwiatkowski *et al.*, 2000). Successful application of the sulfur SAD (S-SAD) technique has been reported using a longer wavelength from a chromium target (Chen *et al.*, 2004; Phillips *et al.*, 2004; Madauss *et al.*, 2004; Rose *et al.*, 2004) with an X-ray apparatus optimized for protein crystallography (Yang *et al.*, 2003). However, the Bijvoet difference is still very small and the development of a highly accurate data collection

method is essential for the routine use of longer wavelength. One of the experimental difficulties in using longer wavelengths is increased X-ray absorption. Although sources of absorption can be minimized by providing an helium beam path and by changing the material of the detector window (Yang *et al.*, 2003; Kitago *et al.*, 2005), a large absorption problem remains for the intensity measurements under cryo-conditions. In the standard crystal mounting method, there is a lens-shaped frozen buffer solution and cryoloop around the crystal. For example, the reduction in intensity is 20% if a thickness of 500μm of water is assumed. This is three times greater than that for Cu *K*α radiation, and results in large variations in scale factors. Taking into account the problems of absorption alone, measuring anomalous signals on the order of 1% is not trivial.

To minimize these absorption effects we have developed a novel technique for mounting a protein crystal to eliminate absorption by the cryobuffer and cryoloop around the frozen crystal (Kitago *et al.*, 2005). This technique increases the accuracy of the anomalous differences between the Bijvoet mates, and makes the in-house S-SAD method with a Cr *K*α X-ray source a very useful tool for high-throughput structure determination. The present study was performed to examine the practical applicability of in-house structure determination using a Cr target and the loopless free crystal mounting method. In addition, a Cr/Cu dual wavelength system that makes it possible to perform a series of structure analyses, from phasing to refinement of the structure in-house is briefly described.

2. Crystal mounting technique for Cr S-SAD method

The new crystal mounting method is based on the easy free crystal mounting method for dehydration of protein crystals reported by Kiefersauer *et al.* (Kiefersauer *et al.*, 2000). They used a micropipette for holding a protein crystal without a loop. The potential disadvantages of their device for routine use for longer wavelength experiments are that a humid air system is necessary to avoid dehydration and the final crystal orientation becomes perpendicular to the micropipette or the phi-axis of the diffractometer. We have overcome these problems by using a micropipette capillary that has a loop at the tip (Kitago *et al.*, 2005). Using this mounting tool, the crystal is kept in the cryo buffer before freezing, which prevents unwanted dehydration, and it can be frozen without buffer and the loop. It is easy to fabricate this mounting capillary. A glass capillary of 1 mm in diameter is pulled to make long taper, then cut and ground at a suitable diameter for each protein crystal. After that, the nylon loop is glued in place carefully aided by use of a microscope. It takes only several minutes to make this mounting capillary if we can use apparatuses for cellular biology such as a micropipette puller, a microforge and a micropipette grinder. The most difficult or annoying part of making this device is glue the nylon loop to the capillary, and an easier method for making this device is under development. The mounting capillary is used as follows: First, a crystal is picked up from the cryo buffer as in the standard cryoloop method. Then, the buffer around the crystal is aspirated through the capillary immediately before the blocked cryostream is flushed for freezing. Finally, the nylon loop is removed with a small hook or forceps under a microscope. Figure 1 shows an example of TT0570 crystal from *Thermus thermophilus* stands on the tip of the capillary. It is possible to mount crystals of different shapes free from buffer and loop using our crystal mounting method. Photographs of the crystals whose structures were solved by Cr SAD are shown in

Figure 2. Movies of the crystal mounting process can be seen at http://castor.sci.hokudai.ac.jp/watanabe/XtalMount/. The success rate of this mounting method becomes close to the standard cryoloop with a few practices. The advantage of the method is that the X-ray absorption can be accounted for by that of the protein crystal itself. Comparison of the data quality of our free mounting method with standard loop mounting has been reported previously (Kitago *et al.*, 2005). As the mounting base used initially was large and it was not possible to store or recover frozen crystals before and/or after exposure, we have developed a modified Hampton CrystalCap Copper with the mounting capillary at its center (Figure 3). With a special magnet base for this cap, it becomes possible to store or recover crystals as with the standard CrystalCap, if necessary. At synchrotron beamlines, this loopless free mounting method also aids analyses of micro crystals that are difficult to center in the lens-shaped frozen buffer in the cryoloop.

The loopless free mounting method has shown to improve data quality for the Cr SAD method. However, it is also attempted to develop an easier crystal mounting method for highly accurate data collection at longer wavelengths. One possibility is the use of laser processing of protein crystals (Kitano *et al.*, 2004; Kitano, Matsumura *et al.*, 2005; Kitano, Murakami *et al.*, 2005). If we can obtain crystals large enough for laser processing, it will be possible to make a perfect spherical crystal as shown in Figure 4 without damage induced by the laser irradiation. These laser shaped crystals also gave us good anomalous signals as the loopless free mounting method (manuscript in preparation).

3. Cr/Cu dual wavelength system

The Cr/Cu dual wavelength system used is a modified Rigaku FR-E SuperBright (2 kW, 60 kV maximum power and voltage, 70 μm x 70 μm focal spot) with a Cr/Cu zebra-stripe target anode, similar to that described by Kwiatkowski *et al.* (2000). It is operated at 40 kV, 40 mA for the Cr target and 45kV, 45mA for the Cu target. Switching between the two wavelengths can be performed easily by rotation of the cathode assembly inside the vacuum chamber. The Osmic Confocal MaxFlux optics optimized for chromium (Cr CMF) are exchanged for the Red optics when using Cu *K*α. This allows use of both wavelengths through one of the two anode ports with a Rigaku R-Axis VII imaging-plate detector. The resolution limit at the edge of the detector imaging plate is 2.2 Å for Cr *K*α, and 1.5 Å for Cu *K*α radiation at a crystal-to-detector distance of 80 mm. To reduce X-ray absorption, the black paper of the detector window of R-AXIS VII was replaced with a carbon-filled thin polymer film. A post-sample helium path and a collimator extension cap were also used to reduce X-ray absorption and scattering by air. A 0.5 mm collimator is used to ensure the whole crystal is always bathed in the X-ray beam. The only disadvantage of our system is that the beam displacement at the phi-axis position between two wavelengths is as large as 7 mm, and alignment of the diffractometer is necessary each time the wavelength is switched. If a second detector is used, it is possible to use Cr *K*α radiation with one of the anode ports and Cu *K*α radiation with the other in alternate shifts to provide an in-house multi-wavelength anomalous diffraction method. The same system is now commercially available as FR-E DW SuperBright with integrated dual-wavelength VariMax mirror.

4. Examples of structure solution by the Cr SAD phasing technique

By use of loopless free crystal mounting method, proteins with molecular weights ranging from 9.6 kDa to 84 kDa have been solved by Cr SAD using native protein crystals without any modifications or derivatizations. Table 1 lists these examples. In all cases the resolution limit of the datasets was 2.2Å, which was limited by the detector dimensions.

Reflections were indexed and integrated with *HKL2000* (Otwinowski & Minor, 1997). The anomalous scattering substructures were solved by *SHELXC* (Sheldrick, 2003) and *SHELXD* (Sheldrick *et al.*, 2001). Primary phasing, phase improvement and auto-model building were performed by *SOLVE* (Terwilliger & Berendzen, 1999), *OASIS* (Hao *et al.*, 2000), *OASIS-2004* (Wang *et al.*, 2004), *DM* (Cowtan, 1994), *RESOLVE* (Terwilliger, 2003b, a), *ARP/wARP* (Perrakis *et al.*, 1999) and *REFMAC* (Murshudov *et al.*, 1997) as shown in Table 1. In all cases except for PH1109 protein, more than 90 % of the structures were automatically built with side chains. Auto-built structures of these examples were shown in Figure 5. Phase improvement using solvent modification is essential for the Cr native SAD method (Watanabe *et al.*, 2005). In the case of the two larger proteins, NCS averaging was also used. Current success rate of our native Cr SAD phasing is 100%, once the dataset is collected with the loopless free crystal mount.

With our dual wavelength system, it is possible to perform a series of structure analyses from phasing to refinement in-house. A partial model built with Cr native SAD can be extended and refined with higher resolution data collected with Cu Kα radiation. For example, the structure of glucosidase with a molecular weight of 84kDa was refined using 1.77 Å Cu dataset to final R/freeR factors of 0.194 and 0.224, respectively.

5. Conclusions

Wang (1985) predicted that the proteins with a Bijvoet ratio of 0.6% would be solved by the SAD method, if accurate dataset were available. From our experience with these proteins solved using our Cu/Cr dual wavelength system and loopless free crystal mounting method, an estimated Bijvoet ratio of 1% is sufficient for a routine native SAD phasing, once well-diffracting crystals are obtained. Actually, a structure of TT0570 protein from *Thermus thermophilus*, whose estimated Bijvoet ratio was 1.09%, was solved without difficulty. Recently, the putative trasncriptional regulator SCO7518 from *Streptomyces coelicolor* A3(2), whose estimated Bijvoet ratio was 0.89%, was also solved using this system (PDB ID: 2DG8). In addition, four of the five examples shown here had extra anomalous scatterers, such as Cl^-, K^+, and Ca^{2+} as shown in Table 1, and these extra scatterers aided phasing. Therefore, the estimated Bijvoet ratio of 1% from the sequence is not a crucial threshold for the native SAD phasing. Bacteria and Archaea have lower frequencies of sulfur-containing residues than eukaryotes as (Micossi *et al.*, 2002). The histograms in Figure 6 show the distribution of estimated Bijvoet ratio of proteins of *P. horikoshii*, *E. coli* and *C. elegans* calculated from the amino acid composition of their ORFs. If the estimated Bijvoet ratio of 1% is enough for the primary phasing, the blue portion of the histogram will be able to be solved with the native SAD method. Using

Cr *K*α radiation and our loopless free mounting method, almost all proteins could be solved in-house without any modifications or derivatizations. This will allow greater flexibility for choosing sample preparation systems.

Figure 1 A TT0570 crystal mounted on the tip of the mounting capillary. The photograph was taken after aspirating the cryo-buffer and freezing. One division of the scale is 50 microns.

Figure 2 Micrographs of crystals solved by the Cr SAD method. (a) PHS023, (b) RNA binding protein, (c) TT0570 and (d) glucosidase.

Figure 3 Modified Hampton CrystalCap for use by the loopless crystal mounting method and magnet base that has a way for aspiration. This modified CrystalCap allows one to store or recover crystals mounted by the loopless method.

Figure 4 Example of the laser processed protein crystal. A lysozyme crystal frozen in the standard cryoloop (a) was laser processed to make a spherical ball-shaped crystal (b). The diameter of the sphere is 250 μm.

Figure 5 Auto-built structures constructed by *ARP/wARP*. (a) PHS023, (b) RNA binding protein, (c) TT0570 and (d) glucosidase. All ribbon models were plotted using *PyMOL* (DeLano, 2002).

Figure 6 Histograms showing the distribution of the number of open reading frames as a function of percentage of the Bijvoet ratio. (a), (b) and (c) are the distribution for Cu *K*α, and (d), (e) and (f) are those for Cr *K*α. (a) and (d) are for *Pyrococcus horikoshii*, (b) and (e) are for *E. coli*, (c) and (f) are for *C. elegans* chromosome I. Columns in which the Bijvoet ratio is higher than 1% are colored blue.

Table 1 Summary of the novel structures solved by the Cr SAD method.

Proteins	PHS023	PH1109	RNA binging protin	TT0570	Glucosidase
No of residues	83	144	241	603	738
Molecular weight	9,667	16,721	26,918	68,624	84,310
Sulfer / molecule	6 Met	4 Met, 2 Cys	4 Met	8 Met, 2 Cys (S-S)	23 Met, 6 Cys
Estimated Bijvoet ratio (%) †	2.45	1.86	1.11	1.09	1.68
Space group	$P3_221$	$P6_522$	$P2_1$	$P2_12_12$	$P2_1$
Unit cell parameters	*a*=61.7, *c*=76.7	*a*=70.0, *b*=144.1	*a*=44.3, *b*=73.9, *c*=44.3, β=109.0	*a*=100.3, *b*=109.0, *c*=114.6	*a*=75.6, *b*=112.4, *c*=102.5, β=100.6
Solvent contents (%)	45.1	58.0	46.5	45.7	51.6
Molecules / AU	2	1	1	2	2
Other	1 K^+	1 Ca^{2+}, 2 Cl^-, 2	2 Cl^-	None	1 Ca^{2+}

Other anomalous scatteres / molecule ‡	1 K^+	1 Ca^{2+}, 2 Cl^-, 2 P	2 Cl^-	None	1 Ca^{2+}
Softwares used	*SHELXD, OASIS, DM, ARP/wARP*	*SHELXD, SHELXE, RESOLVE*	*SHELXD, SOLVE, RESOLVE, OASIS-2004, DM, ARP/wARP*	*SHELXD, SOLVE, RESOLVE, OASIS-2004, DM, ARP/wARP*	*SHELXD, SOLVE, RESOLVE, ARP/wARP*
No of auto-built residues with	154 (93%)	79 (55%) *	223 (93%)	1167 (97%)	1378 (93%)

† Calculated after (Hendrickson & Teeter, 1981) using only sulfur atoms as anomalous scatterers.

‡ Confirmed by final structures.

* in the case of PH1109, we did not use *ARP/wARP* because Coenzyme A binds to the protein.

Acknowledgements This work was done at Hokkaido University in the Prof. Isao Tanaka's laboratory. I would like to thank Yu Kitago for SAD experiments and data process; Naoki Sakai, Min Yao, Yong-Gui Gao, Ayane Morita, Momoyo Kitamura for providing their crystals; Katsumi Tsukamoto of Rigaku for modifying FR-E; SOSHO Project (Crystal Design Project) of Osaka University, SOSHO Inc., and Nikon Corp. for the laser crystal processing. The author is also grateful to Hai-fu Fan for support with OASIS-2004. This study was supported in part by a research grant from the National Project on Protein Structural and Functional Analysis from the Ministry of Education, Culture, Sports, Science, and Technology of Japan.

References

Blow, D. (2003). *Methods Enzymol.* **374**, 3-22.
Chen, L., Chen, L. R., Zhou, X. E., Wang, Y., Kahsai, M. A., Clark, A. T., Edmondson, S. P., Liu, Z. J., Rose, J. P., Wang, B. C., Meehan, E. J. & Shriver, J. W. (2004). *J. Mol. Biol.* **341**, 73-91.
Cowtan, K. (1994). *Joint CCP4 and ESF-EACBM Newsletter on Protein Crystallography* **31**, 34-38.
Dauter, Z., Dauter, M. & Dodson, E. (2002). *Acta Cryst.* **D58**, 494-506.
DeLano, W. L. (2002). *The PyMOL Molecular Graphics System (2002) on World Wide Web http://www.pymol.org*.
Hao, Q., Gu, Y. X., Zheng, C. D. & Fan, H. F. (2000). *J. Appl. Cryst.* **33**, 980-981.
Hendrickson, W. A. & Teeter, M. M. (1981). *Nature* **290**, 107-113.
Kiefersauer, R., Than, M. E., Dobbek, H., Gremer, L., Melero, M., Strobl, S., Dias, J. M., Soulimane, T. & Huber, R. (2000). *J. Appl. Cryst.* **33**, 1223-1230.
Kitago, Y., Watanabe, N. & Tanaka, I. (2005). *Acta Cryst.* **D61**, 1013-1021.
Kitano, H., Adachi, H., Murakami, A., Matsumura, H., Takano, K., Inoue, T., Mori, Y., Owa, S. & Sasaki, T. (2004). *Jpn. J. Appl. Phys.* **43**, L73-L75.
Kitano, H., Matsumura, H., Adachi, H., Murakami, S., Takano, K., Inoue, T., Mori, Y., Doi, M. & Sasaki, T. (2005). *Jpn. J. Appl. Phys.* **44**, L54-L56.
Kitano, H., Murakami, S., Adachi, H., Matsumura, H., Takano, K., Inoue, T., Mori, Y., Doi, M. & Sasaki, T. (2005). *J. Biosci. Bioeng.* **100**, 50-53.
Kwiatkowski, W., Noel, J. P. & Choe, S. (2000). *J. Appl. Cryst.* **33**, 876-881.
Madauss, K., Juzumiene, D., Waitt, G., Williams, J. & Williams, S. (2004). *Endocr. Res.* **30**, 775-785.

Micossi, E., Hunter, W. N. & Leonard, G. A. (2002). *Acta Cryst.* **D58**, 21-28.
Mueller-Dieckmann, C., Panjikar, S., Tucker, P. A. & Weiss, M. S. (2005). *Acta Cryst.* **D61**, 1263-1272.
Murshudov, G. N., Vagin, A. A. & Dodson, E. J. (1997). *Acta Cryst.* **D53**, 240-255.
Otwinowski, Z. & Minor, W. (1997). *Methods Enzymol.* **276**, 307-326.
Perrakis, A., Morris, R. & Lamzin, V. S. (1999). *Nat. Struct. Biol.* **6**, 458-463.
Phillips, J. D., Whitby, F. G., Warby, C. A., Labbe, P., Yang, C., Pflugrath, J. W., Ferrara, J. D., Robinson, H., Kushner, J. P. & Hill, C. P. (2004). *J. Biol. Chem.* **279**, 38960-38968.
Rice, L. M., Earnest, T. N. & Brunger, A. T. (2000). *Acta Cryst.* **D56**, 1413-1420.
Rose, J. P., Liu, Z. J., Tempel, W., Chen, D., Lee, D., Newton, M. G. & Wang, B. C. (2004). *Rigaku J.* **21**, 1-9.
Sheldrick, G. M. (2003). *SHELXC* Göttingen University, Germany.
Sheldrick, G. M., Hauptman, H. A., Weeks, C. M., Miler, M. & Usón, I. (2001). *International Tables for Crystallography* **F**, 333-351.
Terwilliger, T. C. (2003a). *Acta Cryst.* **D59**, 38-44.
Terwilliger, T. C. (2003b). *Acta Cryst.* **D59**, 45-49.
Terwilliger, T. C. & Berendzen, J. (1999). *Acta Cryst.* **D55**, 849-861.
Wang, B. C. (1985). *Methods Enzymol.* **115**, 90-112.
Wang, J. W., Chen, J. R., Gu, Y. X., Zheng, C. D. & Fan, H. F. (2004). *Acta Cryst.* **D60**, 1991-1996.
Watanabe, N., Kitago, Y., Tanaka, I., Wang, J., Gu, Y., Zheng, C. & Fan, H. (2005). *Acta Cryst.* **D61**, 1533-1540.
Yang, C., Pflugrath, J. W., Courville, D. A., Stence, C. N. & Ferrara, J. D. (2003). *Acta Cryst.* **D59**, 1943-1857.

Figure 1.

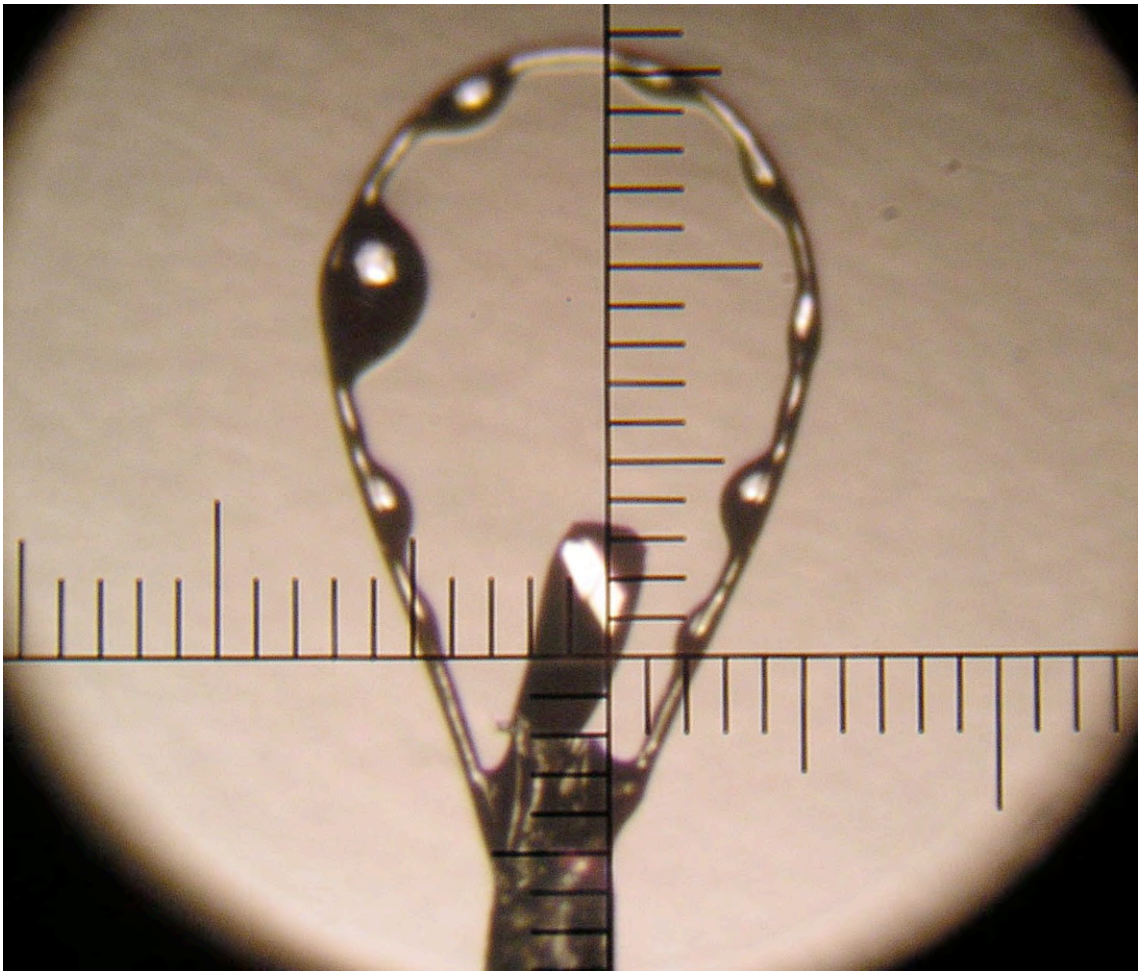

Figure 2.

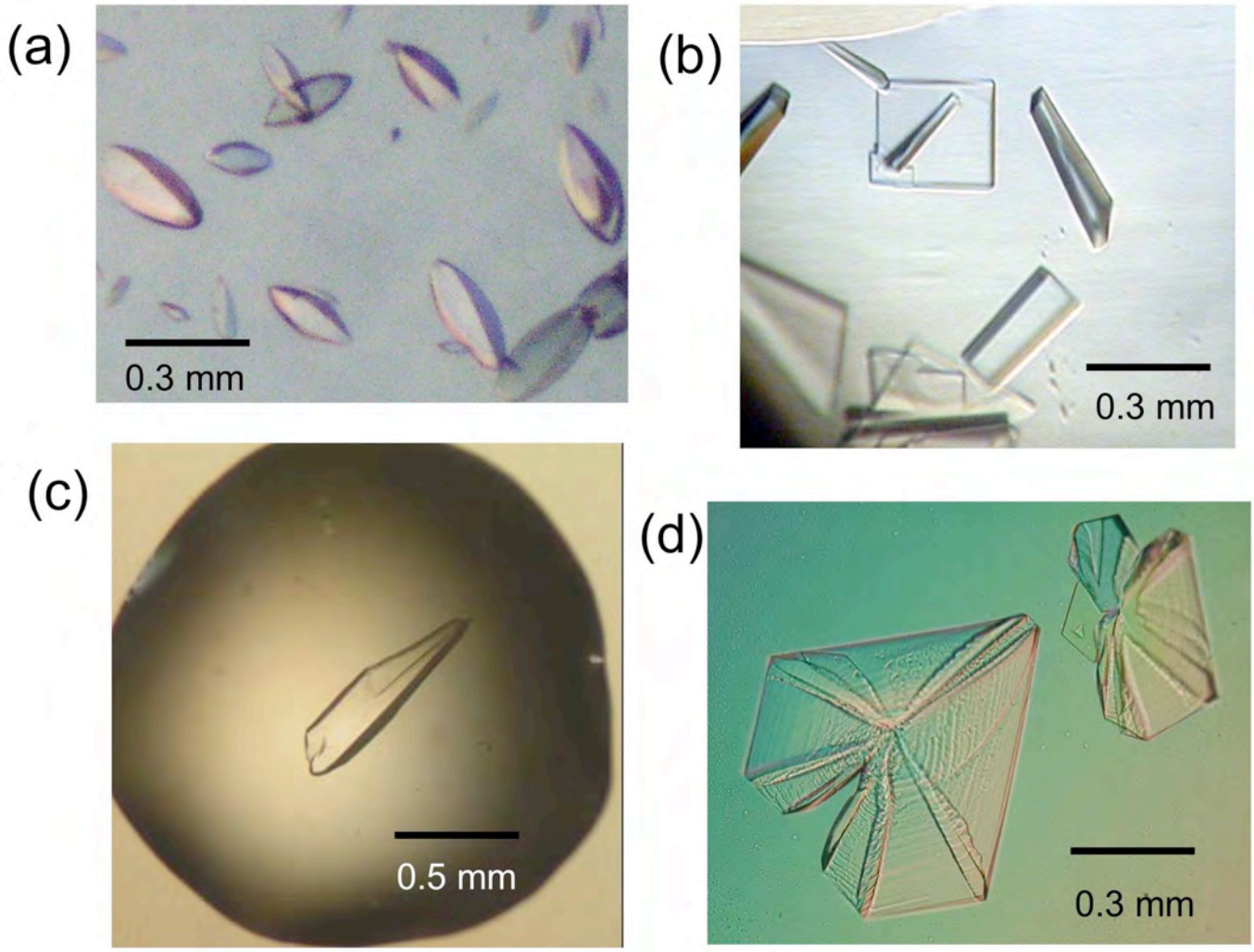

Figure 3.

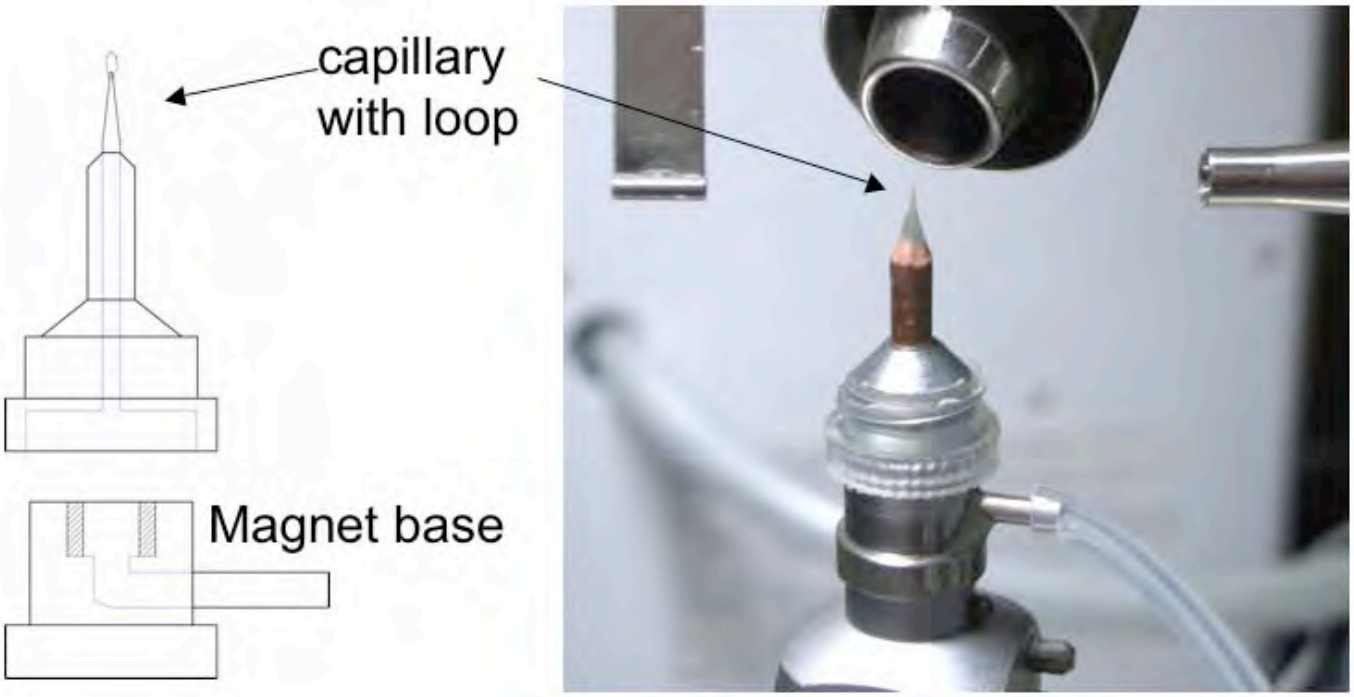

Figure 4.

(a)

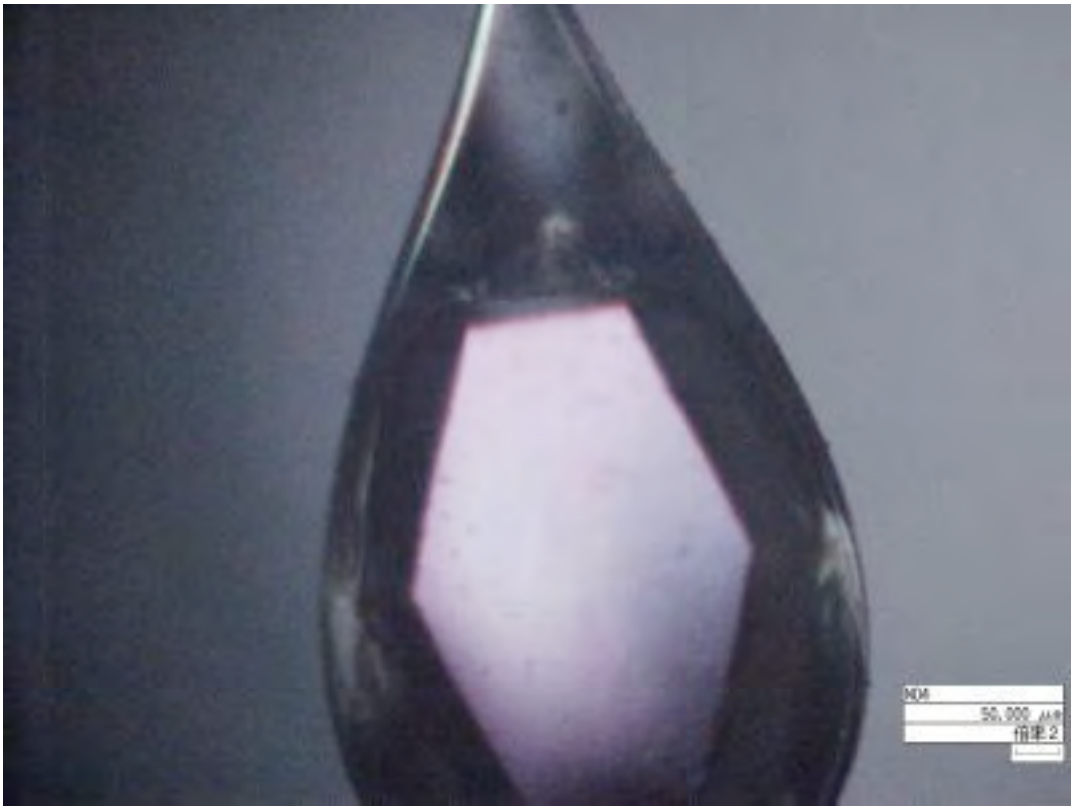

(b)

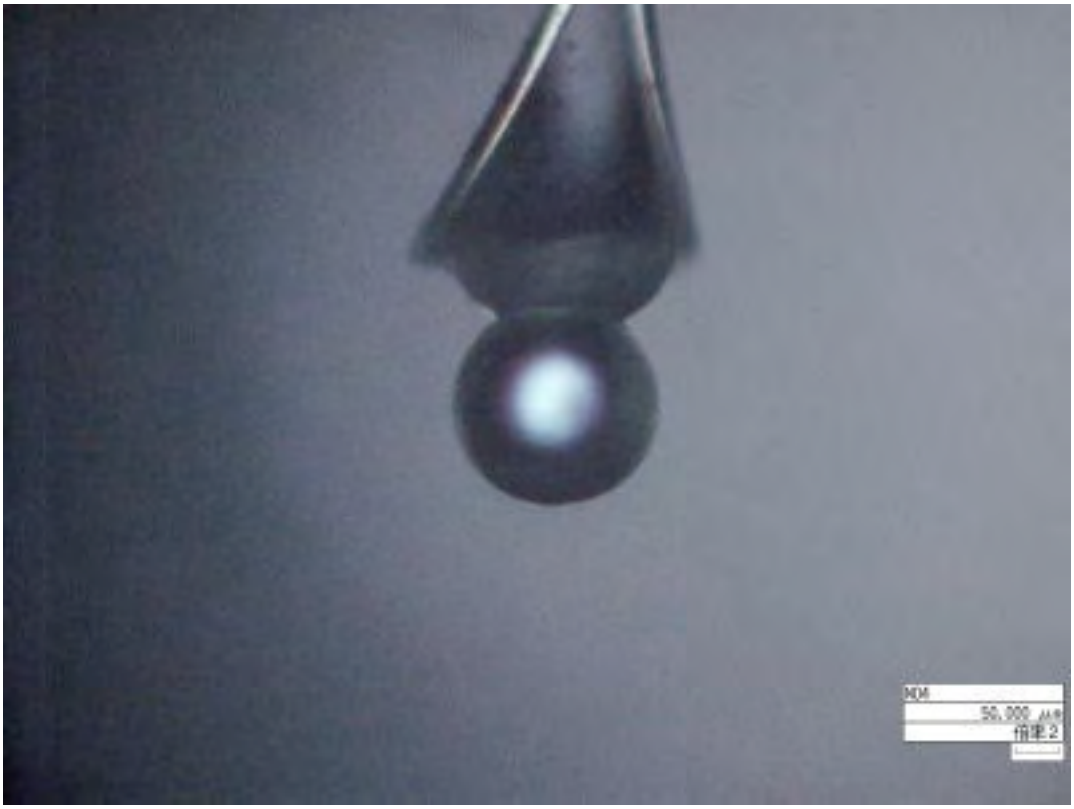

Figure 5.

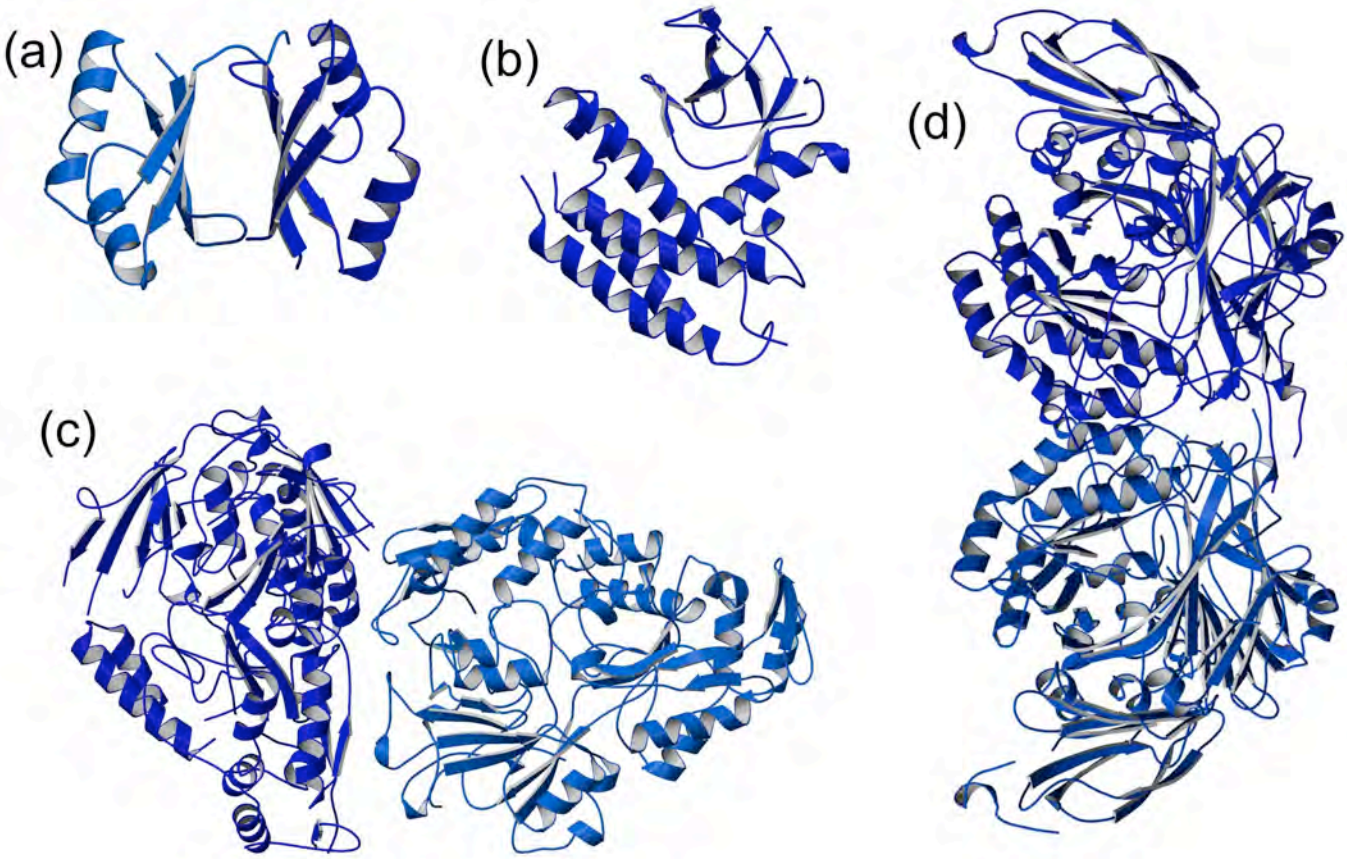

Figure 6.